Journal of Physics: Conference Series **424** (2013) 012003 doi:10.1088/1742-6596/424/1/012003

Helicity dependent meson photoproduction on ^{3}He in the $\triangle$-resonance region.

P. Pedroni[1]
For the CBMAMI and A2 Collaborations

[1] INFN, Sezione di Pavia, Via A. Bassi 6, 27100 Pavia, Italy

E-mail: pedroni@pv.infn.it

Abstract. The first measurement of the helicity dependence of the total inclusive photoabsorption cross section and of partial photon-induced reaction channels on ^{3}He was carried out at MAMI (Mainz) in a photon energy range between 200 and 450 MeV. The experiment used the large acceptance Crystal Ball spectrometer, complemented by a charged particle and a vertex detector, a circularly polarized tagged photon beam and a longitudinally polarized high-pressure ^{3}He gas target. The results obtained give information on the GDH sum rule on the neutron and allow an investigation of the modifications of nucleon properties inside ^{3}He.

1. Introduction

Since the beginning of the 1960s, a central issue of nuclear and particle physics has been the determination of the internal structure of the nucleon, in particular of the spin structure, which is not so well understood as other nucleon properties. For this study, of particular interest are sum rules, which connect information from all energies to fundamental parameters of the present interaction models. The Gerasimov-Drell-Hearn sum rule [1, 2] is a good example of these rules. It relates the nucleon anomalous magnetic moment (AMM) κ , the spin S and the mass M of a nucleon to the integral over the weighted helicity difference of the total absorption cross section for circularly polarized photons on a longitudinally polarized nucleon target. It can be written as:

$$I_{GDH} = \int_{\nu_{th}}^{\infty} \frac{\sigma_p - \sigma_a}{\nu} d\nu = 4\pi^2\kappa^2 \frac{e^2}{M^2} S \ , \tag{1}$$

where ν is the photon energy, α is the fine-structure constant, σ_P and σ_A denote the total absorption cross section for parallel and antiparallel orientation of photon and particle spins, respectively. The lower limit of the integral, ν_0 corresponds to pion production and photodisintegration threshold for a nucleonic and nuclear target, respectively. Table 1 reports the magnetic moment μ and the AMM κ values for protons, neutrons, deuterons and ^{3}He nuclei. The GDH sum rule is derived from very general fundamental physical principles, in particular from the forward Compton scattering, the optical theorem and the low energy theorems. In the past, there have been several attempts to find causes for a failure of the GDH sum rule. The only "weak" hypothesis is the assumption that the Compton scattering becomes spin-independent as the photon energy tends to infinity. Possible explanations for this violation could be the exchange of a_1-like meson between the photon and the nucleon or a non-pointlike quark structure.

Table 1. Magnetic moment μ and AMM κ (units: μ_N, nuclear magneton) for protons, neutrons, deuterons and ^{3}He nuclei.

	p	n	d	^{3}He
μ	2.79	-1.91	0.86	-2.13
κ	1.79	-1.92	0.65	498

The test of this relation then provides a fundamental check of our knowledge of the γ-nucleon interaction, as well as of the physics of strongly interacting systems; it is also a check of the existing photo-reaction models. In addition, through the helicity dependent partial channels, it will be possible to access new observables and to determine the baryon resonance properties.

An estimate of the GDH sum rule value for the nucleon can be evaluated from the existing multipole analyses of the available single pion photoproduction data (mostly from unpolarized experiments) [3, 4] and phenomenological models of multipion and heavy meson photoproduction reactions [5, 6, 7] up to $E_\gamma \simeq 2$ GeV. Above this energy, the contribution can be calculated from Regge-type approaches [8]. Table 2 reports the current theoretical estimates of the GDH sum rule values both for the proton and the neutron. Predictions for the $N\pi$ channels are both from SAID [3] and MAID [4] (within brackets) multipole analyses.

A discrepancy can be clearly seen between these theoretical predictions and the GDH sum rule value for the proton, while the neutron GDH value is roughly reproduced. In addition, it is worth noting that according to the models, I_{GDH} for the proton and the neutron are roughly the same, while this is not the case for the GDH sum rule predictions. In order to find out the reasons for this discrepancy, a precise measurement of the GDH integral for both the proton and the neutron is needed, as well as a systematic study of the partial channels, in particular of the $N\pi(\pi)$ ones, which give the dominant contribution to the GDH integral.

The first experimental check of the GDH sum rule for the proton was performed by the GDH collaboration jointly at the Mainz and Bonn tagged photon facilities, where the I_{GDH} was experimentally evaluated in the photon energy range between 200 MeV and 2.9 GeV [9, 10, 11, 12]. The combination of this result with the theoretical predictions for the unmeasured energy ranges gives an estimated value of the GDH integral of $211 \pm 5(\text{stat}) \pm 12(\text{sys})\mu$b. The obtained result supports the validity of the GDH sum rule for the proton, at odds with the theoretical estimates given in Table 2. This discrepancy is mainly due to the oscillating photon energy dependence of the GDH integrand, due to the alternating sign of the multipole contributions. In order to have a reliable prediction of the GDH integral, a very high accuracy, that has not been reached yet, is needed for the theoretical models.

2. The GDH sum rule for the neutron

In the neutron case, the experimental verification of the GDH sum rule is complicated by the lack of free neutron targets. In order to compensate for this lack, deuteron or high pressure ^{3}He targets can be used. In both cases, nuclear structure effects and final state interactions prevent the direct access to the the free nucleon cross section of and the evaluation of the neutron contribution will be model dependent. The first experimental measurement carried out using longitudinally polarized deuterons has been performed in the energy region between 0.2 and 1.8 GeV by the GDH collaboration [13, 14, 15]. In [15] a very rough estimate was derived for the GDH integral value for the neutron from the combination of these data with the ones from the proton. However, the lack of reliable nuclear models describing in a satisfactory manner the helicity dependent γ -d interactions and the presence of a large proton background contribution,

Table 2. Theoretical estimates of the GDH sum rule values for the proton and the neutron.

	I_{GDH} proton	I_{GDH} neutron
$\gamma N \to N\pi$	172 [164]	147 [131]
$\gamma N \to N\pi\pi$	94	82
$\gamma N \to N\rho$	-8	-6
$\gamma N \to K\Lambda(\Sigma)$	-4	2
$\gamma N \to N\rho(\omega)$	0	2
Regge contribution ($E_\gamma > 2$ GeV)	-14	20
TOTAL	$\sim$ 239 [231]	$\sim$ 247 [231]
GDH sum rule	204	233

prevent at the moment a reliable extraction of the GDH neutron value.

A complementary and more direct access to a free polarized neutron is given by a longitudinally polarized ^{3}He target. While the proton and the neutron inside the deuteron are essentially in s-states of relative motion with aligned spins, ^{3}He is (with $\sim 90\%$ probability) a system consisting of two protons with spins paired off and an active unpaired neutron, in relative s-states. As a result, the spin contribution of the two protons cancels off and the magnetic moment of ^{3}He can be approximated with the magnetic moment of the neutron. Therefore, it is expected that the measured GDH integral for ^{3}He above the pion production threshold will already be a good approximation of the GDH integral value for the neutron. In a PWA approach, and above the pion production threshold, the following formula can then be used:

$$I_{GDH}^{^3He} = p_n \cdot I_{GDH}^{neutron} + p_p \cdot I_{GDH}^{proton} \tag{2}$$

where $p_p = -0.052$ and $p_n = 0.87$ are the are the effective degrees of neutron and proton polarization inside ^{3}He as evaluated by [16]. Since the proton contribution to the measured helicity dependent yields is much smaller than in the deuteron case(for which $p_p = p_n = 0.92$), it can be clearly seen that the most accurate evaluation of I_{GDH} will come from ^{3}He.

In any case, the comparison between the two different free neutron values extracted from both targets using different nuclear models will play a crucial role in constraining the theoretical analyses and will give a fundamental cross check of the reliability of the free neutron extraction procedures.

3. Experimental Set-up

The experiment was carried out at the tagged photon facility of the MAMI accelerator in Mainz. Circularly polarized photons were obtained by bremsstrahlung of longitudinally polarized electrons having an energy of 525 MeV and an average polarization of about 80%. The relative electron polarization was continuously monitored using a Moeller polarimeter and its absolute value was periodically measured using a Mott polarimeter. This parameter was then determined with an absolute accuracy of 3%. The bremsstrahlung photons were tagged using the Glasgow-Mainz magnetic spectrometer with an energy resolution of about 1 MeV [17, 18, 19]. The relative tagging efficiency was monitored throughout the experiment using an ionization chamber which measures the overall photon flux and absolute measurements were regularly made by a total-absorption lead glass counter, which was moved into the beam line at reduced photon intensity.

In this way, the intensity of the tagged photon flux was known with an accuracy of 5% [20].

A high-pressure (∼4 bar) polarized ^{3}He gas target has for the first time been used with a photon beam line. The polarized gas was contained in a cylindrical cell with a total length of 20 cm and an outer diameter of 6 cm. It is made from quartz glass with two 50 μm thick titanium foils as entry and exit windows for the photon beam (see figure 1). These materials were chosen since they provide the necessary gas tightness and give an acceptably long relaxation time of the gas polarization. Under these conditions, the ^{3} He gas target density is relatively low ($\approx 2.5 \cdot 10^{21}$ nuclei/cm^2) compared to that of a solid or liquid target. Despite this, the ^{3}He gas target is pure, so it has a greater fraction of polarized neutron with respect to the deuterated butanol case.

After the polarization process of the gas, performed outside the experimental area using the the Metastability Exchange Optical Pumping (MEOP) method [16], the target cell was inserted into the detector system. There a solenoid provided a very homogeneous guiding magnetic field to maintain the polarization alignment (see figure 2). A relative measurement of the polarization was done every hour using NMR techniques. The principles of operation for this target, as well as the complete target setup used in the experiment are detailed in [22]. The ^{3}He nuclei were polarized typically up to about 70% with relaxation times of about 20 hours. The target density and polarization degree were known with an accuracy of 2% and 5% respectively [22].

The reaction products were detected by a detector system, consisting of the Crystal Ball (CB) NaI spectrometer, complemented by the Multi-Wire Proportional Chambers (MWPCs), used to identify and track the charged particles, and the cylindrical Particle Identification Detector (PID), used to distinguish the charged from the neutral particles detected by the CB (see figure 2). The combined information provided by these three detectors provides accurate energy, angle and particle identification in the azimuthal (ϕ) and polar (θ) angular regions from 0° to 360° and from 21° to 159°, respectively.

Finally, in order to suppress as much as possible the background originating from reactions on the atomic electrons, a threshold Cherenkov detector was installed. The detector was located downstream of the CB detector to cover the polar angular range from 0° to 18°, where nearly all atomic events occur.

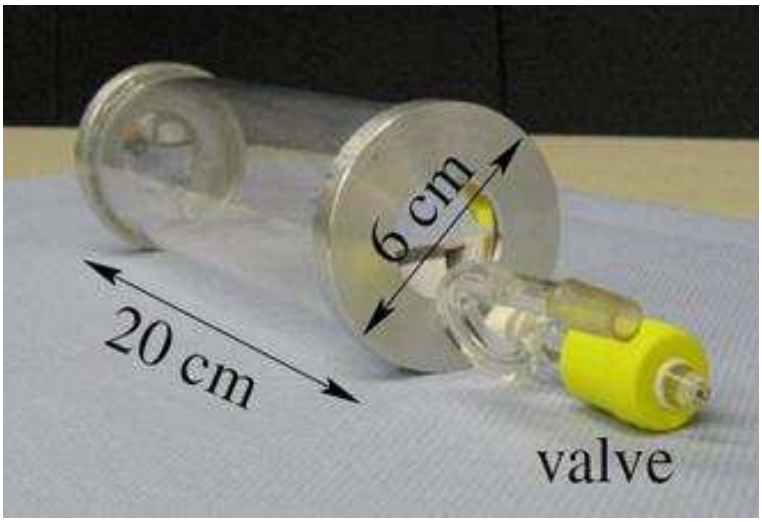

Figure 1. The polarized ^{3}He target cell.

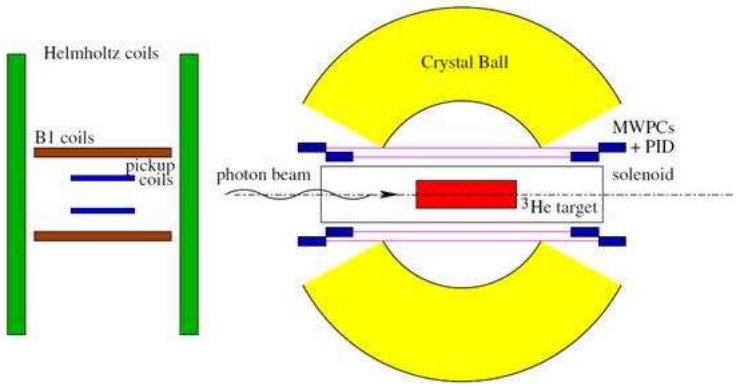

Figure 2. Schematic view of the experimental set-up.

4. Unpolarized data analysis

4.1. Total inclusive cross section (σ_{tot})

To avoid large systematic uncertainties arising from the detection of all single partial reaction channels, an inclusive method of data analysis has been developed to directly determine the total inclusive photoabsorption cross section (see, for instance, [23]). In this method the identification of individual processes is not required; what is necessary is to observe at least one reaction product of all possible hadronic final states with almost complete acceptance, as far as solid angle and efficiency are concerned. The corrections needed to evaluate the detector efficiencies and the loss of events emitted in the angular/momentum regions not covered by the detector have to be kept as low as possible to minimize model dependent contributions. Due to the roughly isotropic distributions of the photo-emitted pions and of the protons coming from photodisintegration in the considered photon energy range, the CB detector, with a very large covered solid angle and an instrinsic detection efficiency greater than about 99% for both charged hadrons and photons coming from neutral meson decays, meets these requirements.

The event selection procedure for the inclusive method was quite simple: at least one cluster (i.e. a group of adjacent hit crystals) was required to be present inside the CB. To further reject e.m. background, only clusters which had a total energy of 40 MeV or higher were used in the analysis. Monte Carlo simulations show that, under these conditions, a large fraction of σ_{tot} (from $\sim$ 90% at E_γ= 200 MeV to $\sim$ 96% at E_γ= 500 MeV) can be directly accessed since, for the dominant quasi-free processes on single nucleons, the minimum pion momenta for the $\pi^{\pm}X$ channels are above the CB detection threshold.

A model dependent extrapolation was evaluated to obtain the remaining part of the total photoabsorption cross section which produces events where all charged hadrons and/or photons from π^0 decay are emitted outside the detector acceptance. The corrections for the $\gamma\ ^3He \rightarrow \pi X$ reactions were evaluated assuming that only quasi-free processes on the single nucleons are present and using the angular distributions for the $\gamma N \rightarrow \pi N$ reactions were evaluated processes predicted by the MAID [4] multipole analysis. The missing contribution from the the $\gamma\ ^3He \rightarrow ppn$ channel has been evaluated taking into account that the dominant reaction mechanism is the absorption on a correlated (n,p) pair. The systematic uncertainty associated to the simplified models used to evaluate the extrapolation corrections is estimated to be 10% of the calculated correction. The combination of all different sources, gives an overall systematic error of about 6% of σ_{tot}.

In figure 3 the values of the unpolarized total inclusive cross section obtained from the present experiment after the subtraction of the empty target spurious contributions [24] are compared to

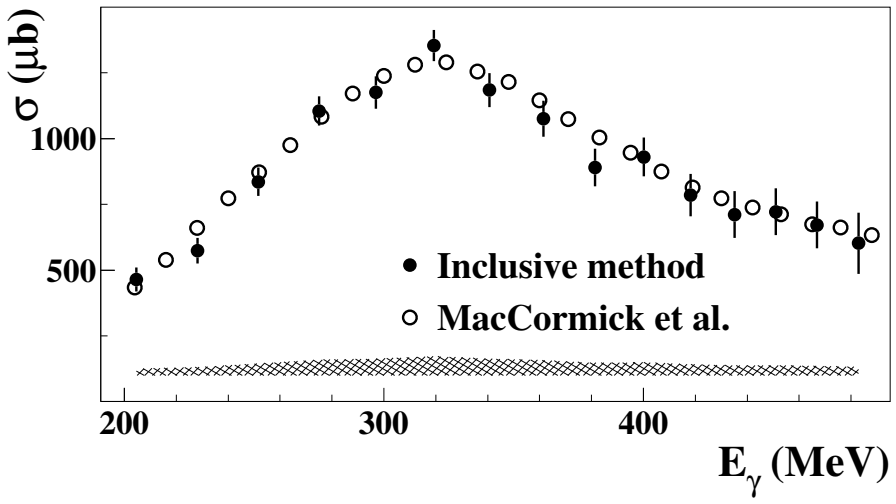

Figure 3. The unpolarized total inclusive photoabsorption cross section on ^{3}He (full circles) is compared to the unpolarized results obtained by the DAPHNE collaboration (open circles) [23].

previous results [23]. The good agreement that can be clearly seen with respect to the published data gives confidence in the total inclusive procedure.

4.2. Partial reaction channels

In order to provide additional experimental information, the particle identification capabilities of the experimental apparatus were used to evaluate the total cross section for the semi-exclusive processes (i) $\gamma\ ^3\mathrm{He} \rightarrow \pi^0 X$ ($\sigma_{\pi^0 X}$), (ii) $\gamma\ ^3\mathrm{He} \rightarrow \pi^{\pm} X$ ($\sigma_{\pi^{\pm} X}$), and for the photodisintegration reaction (iii) $\gamma\ ^3\mathrm{He} \rightarrow ppn$ (σ_{ppn}). All these cross sections have not been measured yet.

The yield from (i) was evaluated by selecting events having two or three neutral clusters in the CB and the π^0 mesons were identified by a standard invariant mass analysis. The main parasitic reactions that can contaminate the data are the $\gamma\ ^3\mathrm{He} \rightarrow \pi^0\pi^0 X$ channels. For this reason, the data analysis was limited to $E_\gamma < 450$ MeV, a region where this contribution is small. The residual contamination was evaluated assuming the dominance of the quasi-free $\gamma N \rightarrow \pi^0\pi^0 N$ reactions and using the measured unpolarized cross section values for these processes previously measured by the GDH [25, 26, 27] and TAPS [28] collaborations.

For this and for the other partial channels, the extrapolation correction have been evaluated as previously explained for the total inclusive method. The systematic uncertainty associated to the event selection procedure and to the efficiency corrections was evaluated to be 3% of the measured yield [20]. The addition in quadrature of all the different sources of systematic uncertainties gives an overall systematic uncertainty of about 7% of the measured reaction yield. The obtained results are shown in figure 4a and compared to the predictions of the Fix-Arenhovel (FA) model (solid line) and of a very simple (VS) model based on the MAID multipole analysis (dashed line) [24]. The FA model is a straightforward extension of the work previously done on the deuteron [30]. The elementary production operator $\gamma N \rightarrow \pi N$ is taken from the MAID multipole analysis and is afterwards embedded into the wave function to take into account the nuclear effects. Empirical attenuation factors were then applied to take into account the absorption of the photoemitted particles inside the nuclear medium. On the contrary, in our VS model it naively assumed that all nucleons inside ^{3}He behave as if they were free. As it can be clearly seen from the difference between these two models, the predicted role of the nuclear effects result in damping and broadening the peak corresponding to the $\Delta(1232)$ resonance excitation.

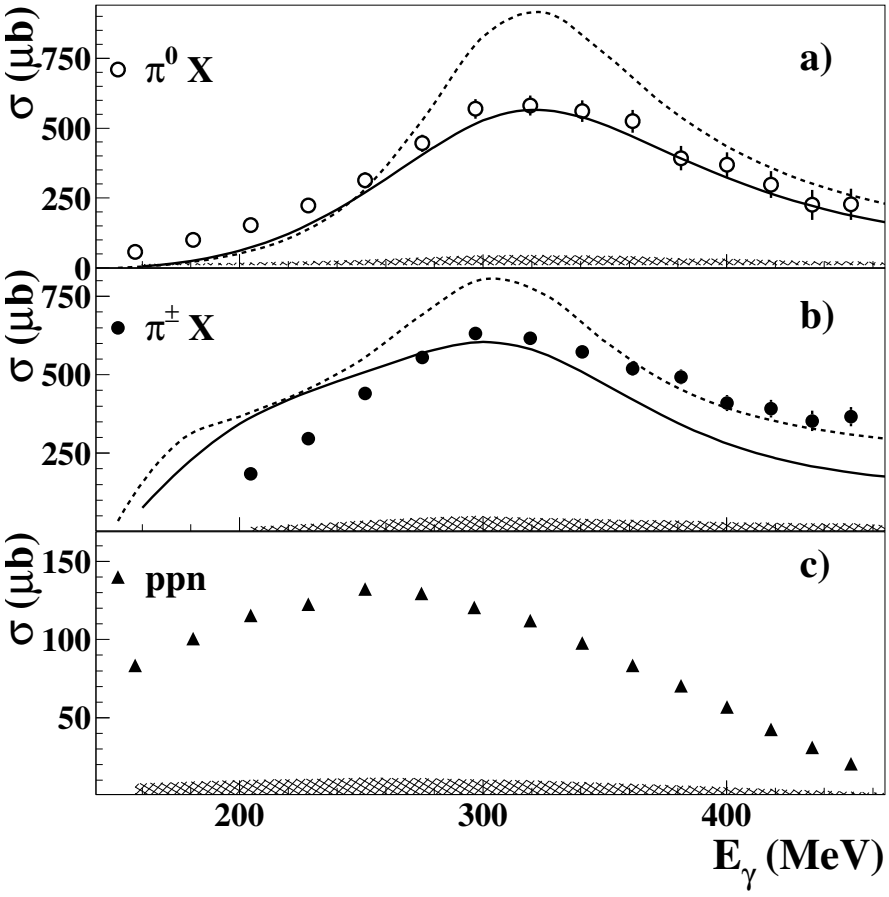

Figure 4. The unpolarized total cross section for a) γ ^{3}He $\rightarrow \pi^0 X$ b) γ ^{3}He $\rightarrow \pi^{\pm} X$ and c) γ ^{3}He $\rightarrow ppn$. The error bars are statistical and the hatched bands show the systematic uncertainties. In a) and b) the experimental data are compared to the FA model (solid line) and to our VS model (dashed line).

Proton and charged pions hitting the CB were identified by a standard $dE/dX - E$ analysis, using the energy information from CB, PID and the direction information from MWPCs [20]. In both cases, software cuts on the interaction vertex coordinates of the selected events allowed a suppression of a large fraction of the events originating from the target walls and windows [22]. The trajectory reconstruction efficiency was directly determined from the experimental data since a part of the $\pi^{\pm}$ events can be discriminated using the approximate angular information given by CB alone instead of the one given by MWPCs. This efficiency was then determined by measuring the fraction of such events that have a reconstructed trajectory using MWPCs information and was found to be about 85% (95%) for $\pi^{\pm}$ (protons) with a smooth dependence on the incident photon energy. An absolute systematic uncertainty of 3% has been estimated on this parameter.

Events from reaction (ii) were obtained by requiring one charged pion being identified in CB. In a similar way as before, the data analysis was limited to $E_{\gamma} < 450$ MeV and the small contamination due to the γ ^{3}He $\rightarrow \pi^+\pi^- X$ channels was evaluated from the $\gamma p \rightarrow \pi^+\pi^- p$ cross section measured by the GDH collaboration [29]. The systematic uncertainty associated to the event selection procedure and to efficiency corrections was evaluated to be 3% of the measured

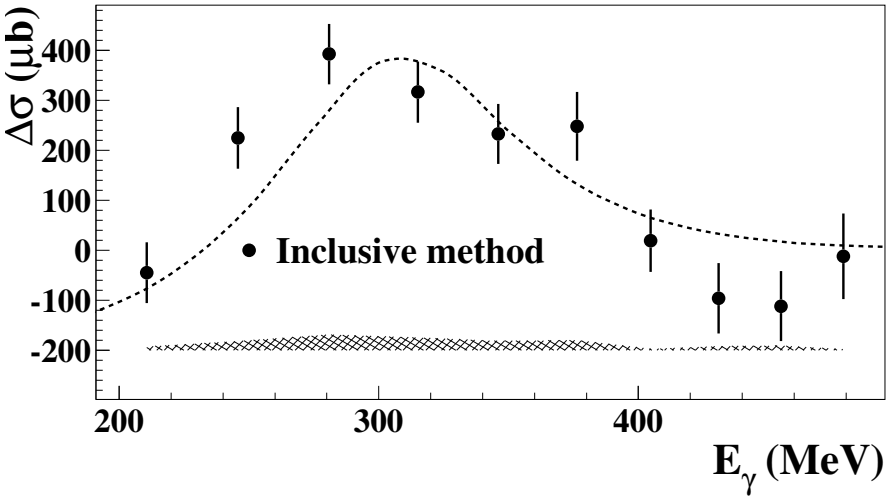

Figure 5. The polarized total inclusive cross section on ^{3}He ($\Delta\sigma_{tot}$) (full circles) compared to the predictions of our VS model (dashed line). The error bars are statistical and the hatched band shows the systematic uncertainties.

yield. The addition in quadrature of all the different sources of systematic uncertainties gives an overall systematic uncertainty of about 7% of the measured reaction yield.

The obtained results are shown in figure 4b and compared to the predictions of the FA model (solid line) and of our VS model [24]. In this case the FA model does not well reproduce our data which for to $E_\gamma > 350$ MeV are very close to our simple model.

The yield from reaction (iii) was evaluated by selecting events having one or two protons identified in CB. Since the major competing background is due to the $\gamma\ ^3\mathrm{He} \rightarrow ppn\pi^0$ reaction, the presence of less than two neutral clusters detected inside CB in coincidence with the proton(s) was also required. The residual background was evaluated from the missing mass spectrum $\gamma\ ^3\mathrm{He} \rightarrow p(p)X$ and subtracted accordingly. The addition in quadrature of all the different sources of systematic uncertainties gives an overall systematic uncertainty of about 8% of the evaluated reaction cross section. The resulting total unpolarized cross section is shown in figure 4c [24]. In this case no specific model is available for comparison.

5. Polarized results and comments

In the analysis of the helicity dependent data, all previously mentioned analysis methods were used to evaluate the difference $\Delta\sigma = (\sigma_p - \sigma_a)$. In this case the contributions from all non-polarized materials present in the target cell vanish. In a similar way as before, the extrapolation correction for $\gamma\ ^3\mathrm{He} \rightarrow \pi X$ was evaluated using the MAID predictions while the $\Delta(pn)$ contribution was calculated using the predictions of the SA model.

The analysis procedure described above results in the helicity dependent total inclusive cross section $\Delta\sigma_{tot}$ as depicted in figure 5 [24] in comparison with the predictions of our VS model, where it was again assumed that the nucleons inside ^{3}He behave as free ones. Only the effects on the nucleon spin alignments due to the ^{3}He s' and d-state probabilities have been taken into account according to equation 2. The agreement between our data and the VS model is reasonable, taking into account the non-negligible statistical experimental errors. This is a hint that nuclear effects are less important than in the unpolarized case.

The total helicity dependent cross sections $\Delta\sigma$ for the (a) $\pi^0 X$, (b) $\pi^\pm X$ and (c) ppn channels are shown in figure 6 together with the corresponding predictions of the FA (solid line) and VS

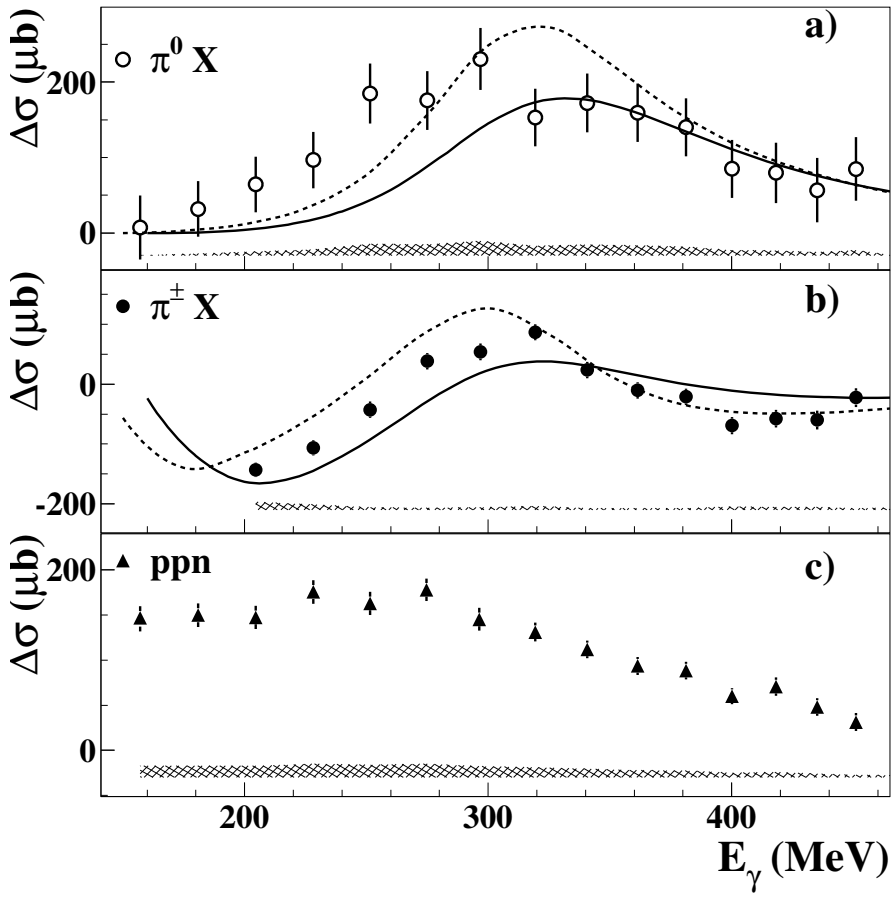

Figure 6. The polarized total cross section for the a) γ ^{3}He $\rightarrow \pi^0 X$ b) γ ^{3}He $\rightarrow \pi^\pm X$ and c) γ ^{3}He $\rightarrow$ *ppn*. The error bars are statistical and the hatched bands show the systematic uncertainties. In a) and b) the experimental data are compared to the FA model (solid line) and to our VS (see eq. 2) model (dashed line).

(dashed line) model [24]. As in the unpolarized case the FA model fairly well reproduces the γ ^{3}He $\rightarrow \pi^0 X$ data only at higher photon energies and it does not reproduces the shape of the γ ^{3}He $\rightarrow \pi^\pm X$ data. Our VS model well reproduces the data at higher photon energies for both reactions. This is a further confirmation that the effects more directly related to the composite nuclear target structure do not have a strong helicity dependence and their net effect is then reduced in the $\Delta\sigma$ case.

6. Conclusions

The helicity dependence of the total inclusive photoabsorption cross section on ^{3}He and both the unpolarized and the helicity dependent cross sections of the partial reaction channels γ ^{3}He $\rightarrow \pi^0 X$, γ ^{3}He $\rightarrow \pi^\pm X$ and γ ^{3}He $\rightarrow$ *ppn* have been measured for the first time at MAMI (Mainz) in the energy region $200 < E_\gamma < 450$ MeV. All these new data provide a very powerful tool to further improve the models for the photoreactions on ^{3}He in the Δ resonance region. Available state-of-the-art calculations are not able to describe in a s atisfactory manner both the unpolarized and the helicity dependent cross section for the πX channels while no model is at present available for the *ppn* channel. This fact strongly motivates further theoretical and

experimental research in the field. In order to pin down the origin of these discrepancies the analysis of both the unpolarized and polarized differential cross sections for the $\gamma\ ^3\mathrm{He} \to \pi^0 X$ and $\gamma\ ^3\mathrm{He} \to \pi^{\pm} X$ is underway.

References

[1] Gerasimov S B 1966 *Sov. J. Nucl. Phys.* **2** 430
[2] Drell S D and Hearn A C 1966 *Phys. Rev.* **96** 1428
[3] Arndt R A et al 2002 *Phys. Rev.* C **66** 055213
[4] Drechsel D et al 2001 *Phys. Rev.* D **63** 114010
[5] Fix A and Arenhövel H 2005 *Eur. Phys. J.* A **25** 115
[6] Sumowigado S and Mart T 1999 *Phys. Rev.* C **60** 028201
[7] Zhao Q, Al-Khalili J S and Bennhold C 2002 *Phys. Rev.* C **65** 032201
[8] Bianchi N and Thomas E 1999 *Phys. Lett.* B **450** 439
[9] Ahrens J et al 2000 *Phys. Rev. Lett.* **84** 5950
[10] Ahrens J et al 2001 *Phys. Rev. Lett.* **87** 022003
[11] Dutz H et al 2003 *Phys. Rev. Lett.* **91** 192001
[12] Dutz H et al 2004 *Phys. Rev. Lett.* **93** 032003
[13] Dutz H et al 2005 *Phys. Rev. Lett.* **94** 162001
[14] Ahrens J et al 2006 *Phys. Rev. Lett.* **97** 202303.
[15] Ahrens J et al 2009 *Phys. Lett.* B **672** 328
[16] et al 1990 *Phys. Rev.* C **42** 2310
[17] Anthony I et al 1991 *Nucl. Instrum. Methods Phys. Res., Sect.* A**301**, 230
[18] Hall S J et al 1996 *Nucl. Instrum. Methods Phys. Res., Sect.* A**368**, 698
[19] McGeorge J C et al 2008 *Eur. Phys. J.* A **37** 129
[20] Schumann S et al 2010 *Eur. Phys. J.* A **43** 269
[21] Colegrove F et al 1963 *Phys. Rev.* **132** 2561
[22] Krimmer J et al 2011 *Nucl. Instrum. Methods Phys. Res., Sect.* A**648**, 35
[23] Mc-Cormick et al 1996 *Phys. Rev.* C **53** 41
[24] Aguar-Bartolomé et al, submitted to *Phys. Lett.*B
[25] Ahrens J et al 2003 *Phys. Lett.*B **551** 49.
[26] Ahrens J et al 2005 *Phys. Lett.*B **624** 173.
[27] Ahrens J et al 2011 *Eur. Phys. J.* A **47** 36.
[28] Kotulla M et al 2005 *Phys. Lett.*B **578** 63.
[29] Ahrens J et al 2007 *Eur. Phys. J.* A **34** 11.
[30] Fix A and Arenhövel H 2005 *Phys. Rev.* C **72** 064004